

THE FLAPPING AIRCRAFT DYNAMICS WITH WING DEFORMATION UNDER GUST INPUT

Kenjiro Okumura*, Hiroshi Tokutake*

***Kanazawa University**

ken0621@stu.kanazawa-u.ac.jp; tokutake@se.kanazawa-u.ac.jp

Keywords: *Flapping aircraft, Wing deformation, Gust response*

Abstract

Aerodynamic forces during flapping flight are affected by changes in the angle of attack due to deformation of the wing. In this study, stability derivatives of the flapping aircraft subject to disturbance input were derived, and the dynamics was modeled with the wing deformation. The control performances were investigated by varying the design parameters. The results showed the optimal elasticity parameters and feedback gain. This paper proposes the concept for a real-time modeling method based around a flapping wing. Fundamental experiments were performed and the concept was validated.

Nomenclature

a	lift slope
A_x, A_z	amplitudes of horizontal and longitudinal flapping motions
A_{x0}, A_{z0}	centers of horizontal and longitudinal flapping motions
c	chord length of wing
C_L	lift coefficient
C_p	pressure coefficient
d	distance between leading edge and center of rotation axis
dm	pitching moment at wing element
e	position of elastic axis
f	frequency
G	torsional stiffness
I_{yy}	moment of inertia about the y -axis
J	cost function
K	feedback gain
L	length of plate

m	mass of the flapping micro air vehicle
M	pitching moment
M_w	aerodynamic moment of wing element
r	position of span direction
R	length of flapping wing
T_s	simulation time
U	velocity of translational motion
U_0	velocity of free stream
v_z	longitudinal flight velocity
V	velocity of wing
V_x, V_z	horizontal and longitudinal velocities of wing
w	complex velocity potential in cylindrical coordinates
w_x, w_z	gusts in horizontal and longitudinal directions
W	complex velocity potential in non-inertial coordinates
x_0	position of rotation axis
z	complex coordinate in wing plane
z_w	position of wake vortex at complex coordinate in wing plane
α	angle of attack
Γ, Γ_w	vorticities of bound and wake vortices
δ	control input
ζ	complex coordinate in circle plane
ζ_w	position of wake vortex at complex coordinate in circle plane
θ	angle of torsion
ρ	atmospheric density
ω	feathering angle rate

Superscripts

* complex conjugate value

1. Introduction

Flapping micro air vehicles (MAVs) can hover as well as rotor aircraft can. Therefore, they can be used as monitoring devices. In order to design high-performance flapping MAVs, analysis of their flight dynamics under actual conditions is necessary.

The aerodynamic performance of a flapping MAV is affected by the torsional deformation and gust input. The flight dynamics should be modeled under the deformation of the wing and disturbances to evaluate the flight control performance. However, only a few studies have been conducted for investigating the flight dynamics of flapping MAVs [1-6]. In the present study, therefore, flight performance was analyzed under gust input with wing deformation. The aerodynamic forces of an aeroelastic flapping wing and the responses to the gust input were formulated. The performance of the feedback control of the flapping aircraft was then studied.

High-performance flight can be achieved if the feedback control can use information on the gust input and aerodynamics forces. Thus, this paper proposes a basic concept for real-time modeling of the flow condition around a flapping aircraft. The numerical calculations for the flapping wing have been reported previously [7]. These previous studies aimed to analyze the fluid dynamics. In contrast, our aim was the real-time calculation of the flow conditions around flapping wing aircraft and its application to feedback control. In order to decrease the calculation time, the potential theory and vortex shedding method [8-10] were used. An asymptotic algorithm using the measured flow condition was constructed for improving the calculation precision. This paper presents the fundamental results for the flat wing and the validation of the proposed method.

2. Flight model with aeroelasticity

2.1 Aerodynamic forces with wing deformation

Figure 1 shows the flight model of a flapping MAV.

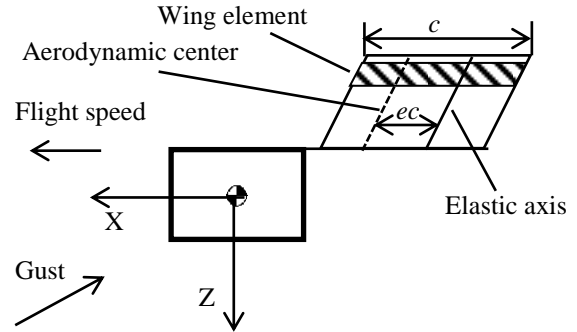


Fig.1 Flight model

The averaged aerodynamic forces in a period of flapping motion were formulated based on the quasi-steady assumption.

The flapping wing was assumed to be a cantilever rectangle aeroelastic wing (Fig.2).

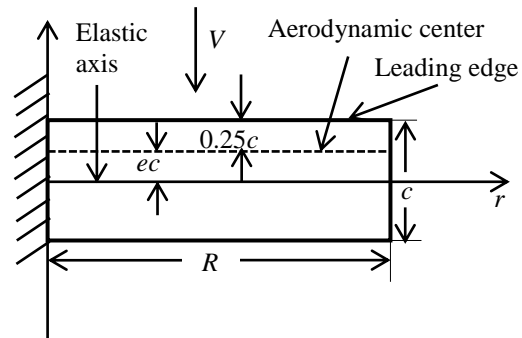


Fig.2 Cantilever wing

The cantilever wing deforms around the elastic axis. Aerodynamic forces generated by the flapping flight are loaded uniformly on the aerodynamic center line. The aerodynamics forces were assumed to balance with the elastic forces. The elastic moment around the elastic axis is related to the aerodynamics moment M_w as follows:

$$\frac{d}{dr} \left(G \frac{d\theta}{dr} \right) = -M_w \quad (1)$$

Here, G is the torsional stiffness. M_w is formulated as follows:

$$M_w = \frac{l}{2} \rho V^2 a (\alpha - \Delta\alpha + \theta) \times ce \quad (2)$$

Here, V is the wind velocity on the wing element and $\Delta\alpha$ is the variation in the angle of attack by the gust input. The angle of torsion is approximated as a quadratic equation:

$$\theta = a_1 r^2 + a_2 r + a_3 \quad (3)$$

The boundary conditions are $\theta = 0$ at $r = 0$ and $d\theta/dr = 0$ at $r = R$. From the boundary conditions, Eq. (3) becomes

$$\theta = a_1 r^2 - 2a_1 R r \quad (4)$$

From Eqs. (1) and (2), the following equation is obtained:

$$\frac{d}{dr} \left(G \frac{d\theta}{dr} \right) + \frac{1}{2} \rho V^2 c^2 e a (\alpha - \Delta\alpha + \theta) = 0 \quad (5)$$

The parameter of the angle of torsion, a_1 , is determined to satisfy Eq. (5) at the point $r = R/2$. Consequently,

$$\theta = \frac{-4V^2 \left(\frac{R}{2}, t \right) c^2 e a (\alpha - \Delta\alpha)}{16G - 3\rho V^2 \left(\frac{R}{2}, t \right) c^2 e a R^2} (r^2 - 2Rr) \quad (6)$$

is obtained. Here, $V(r, t)$ is the wind velocity at the spanwise position r and time t . Eq. (6) is used to calculate the aerodynamic force of the wing element. The aerodynamic moment of the wing element becomes as follows:

$$dm(r, t) = \rho c a V^2 \left[\alpha + \theta - \left\{ \tan^{-1} \left(\frac{V_z}{V_x} \right) - \tan^{-1} \left(\frac{V_z - w_z}{V_x + w_x} \right) \right\} \right] \times \left\{ \cos \left(\frac{V_z}{V_x} \right) \right\} x dr \quad (7)$$

The stability derivatives subject to disturbance input under wing deformations were analyzed. In this study, aerodynamic forces were formulated under the assumption of steady, straight flight. The flight parameters are listed in Table 1. The stability derivatives of pitching moment subject to the longitudinal disturbance input $\partial M / \partial w_z$ were calculated from the averaged aerodynamic moment as follows:

$$M(w_x, w_z) = \frac{1}{T} \left(\int_0^T \int_0^R dm(r, t) dr dt \right) \quad (8)$$

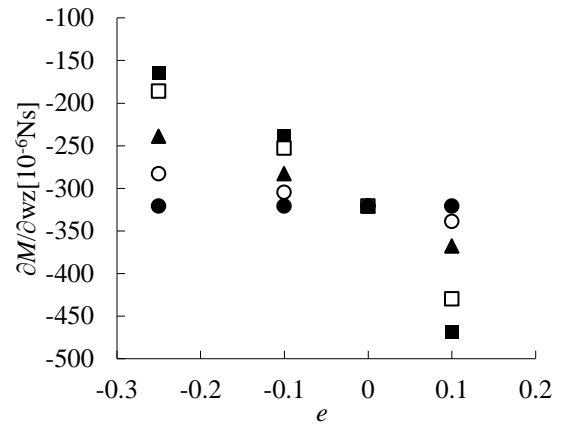
$$\frac{\partial M}{\partial w_z} \cong \left(\frac{M(0, dw_z) - M(0, 0)}{dw_z} \right) \quad (9)$$

Figure 3 shows the relationship between the stability derivative and the elastic parameter e for several values of torsional stiffness G .

When the torsional stiffness was small, the disturbance response was large. This tendency was strong when the torsional stiffness was small.

Table1 Flight simulation parameters

parameters	values
a	2π
A_x, A_z [rad]	$\frac{33\pi}{180}, \frac{\pi}{4}$
A_{x0}, A_{z0} [rad]	$\frac{\pi}{6}, 0$
c [m]	14.2×10^{-3}
f [s^{-1}]	15.0
G [$N m^2$]	1.00×10^{-5}
I_{yy} [$kg m^2$]	241×10^{-9}
m [kg]	1.92×10^{-3}
R [m]	46.7×10^{-3}
U_0 [$m s^{-1}$]	5.45
ρ [$kg m^{-3}$]	1.20



■ $G = 0.800 \times 10^{-5}$ [Nm^2] □ $G = 1.00 \times 10^{-5}$ [Nm^2]
 ▲ $G = 2.00 \times 10^{-5}$ [Nm^2] ○ $G = 3.00 \times 10^{-5}$ [Nm^2]
 ● $G = \infty$ [Nm^2]

Fig.3 Stability derivative and elasticity parameter

2.2 Flight dynamics of flapping aircraft

Linearized equations of motion of the flapping aircraft were constructed, and the characteristics of the flight dynamics were analyzed. Table 2 lists the eigenvalues with the variations in the elastic axis position.

These flight dynamics were unstable for all values of e ; the further back the placement of the elastic axis from the wing, the more

aggressive the divergence of the dynamics became. These results indicate that feedback control is required.

Table2 Eigenvalues

e	Eigenvalues of flight model
-0.250	-0.720±0.807i, 6.87, -5.95
0	-23.4,-0.035, 18.8, 3.76
0.100	-30.4,-0.980, 24.4, 4.64

2.3 Flight control

A simple feedback control using the position of the stroke plane as a control input was constructed. This control input generates only the pitching moment. Figure 4 shows the block diagram of this control system.

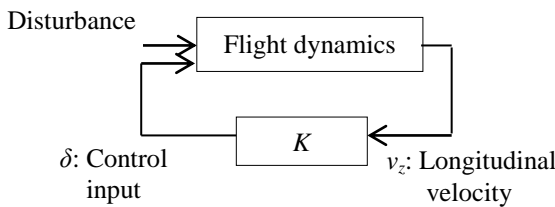


Fig.4 Block diagram

The responses to the longitudinal disturbance were simulated, and the performance of the feedback control was evaluated by the following cost function:

$$J = \frac{1}{T_s} \int_0^{T_s} v_z^2 dt \quad (10)$$

The results are shown in Fig.5

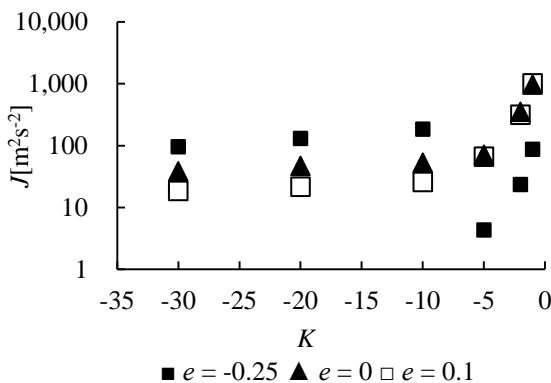


Fig.5 Feedback gain and control performances

When the absolute value of the feedback gain K was small, the control performance improved the further forward the elastic axis was placed. However, when the absolute value of K was large, the control performance improved the further back the elastic axis was placed. In this parametric study, the optimal solution for the flapping MAV design was to place the elastic axis of the flapping wing at the leading edge with a small absolute value of the feedback gain.

3. Calculation of unsteady aerodynamic forces

3.1 Real-time modeling concept

The flow condition around a flapping wing is useful for feedback control. However, it is difficult to measure the flow condition at many points directly. Thus, the concept of real-time calculation of the flow condition around the flapping wing is proposed; the algorithm corresponding to this concept includes the following steps.

- (i) The initial boundary condition is defined.
- (ii) The flapping aircraft motion is measured.
- (iii) The measured aircraft motion is input to the flow model, and the flow condition is calculated.
- (iv) The flow conditions at several points on the surface are measured and compared with the value estimated from the flow model.
- (v) The estimation error of the flow condition is used to update the boundary condition.
- (vi) Return to step (ii).

A simple flow model is required to perform this algorithm in real time. Therefore, the potential method based on shedding vortices was used [8-10]. Although, this method is very simple, it cannot be used to express complicated flow. The estimated flow condition is improved by using the estimation error asymptotically.

3.2 Theory

As a first step of the real-time modeling, the aerodynamics forces of a flapping flat plate wing were calculated by the potential theory and

the vortex shedding method [8-10] and compared with the experimental results. This theory is explained in brief below.

In the complex plane $z(x,y)$, the x axis corresponds to the chord direction of the plate and the origin corresponds to the rotation axis (Fig.6).

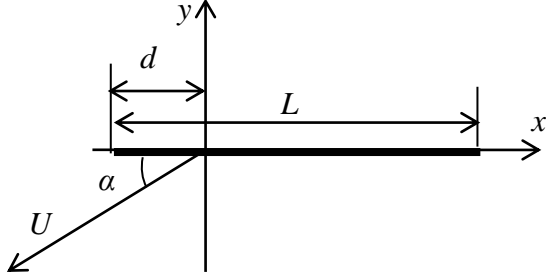


Fig.6 Schematic sketch of the plate

Two-dimensional aerodynamic forces are evaluated in a non-inertial frame. The Joukowski conversion

$$z(\zeta) = x_0 + \zeta + \frac{a^2}{\zeta} \quad (11)$$

is applied. The complex velocity potential is determined as follows:

$$w(\zeta) = -U^*(t)\zeta - U(t)\frac{a^2}{\zeta} + \frac{i\omega}{2}(\zeta + x_0)^2 - \frac{i\omega}{2}\left(\frac{a^2}{\zeta} + x_0\right)^2 + \frac{\Gamma_w}{2\pi i} \ln(\zeta - \zeta_w) - \frac{\Gamma_w}{2\pi i} \ln\left(\zeta - \frac{a^2}{\zeta^*}\right) + \frac{\Gamma_w + \Gamma}{2\pi i} \ln(\zeta) \quad (12)$$

Unsteady aerodynamic forces can be obtained using the following equation [8]:

$$F_x - iF_y = \frac{i\rho}{2} \oint_B \left(\frac{dW}{dz}\right)^2 dz + i\rho \frac{\partial}{\partial t} \left[\oint_B W dz \right]^* \quad (13)$$

The bound vortex strength and wake vortex strength are calculated under the Kutta condition and Thomson's circulation theorem. The position of the wake vortex is determined as follows:

$$z_w(t + \Delta t) = z_w(t) + \left(\frac{dW}{dz}\right) dt \quad (14)$$

3.3 Calculation method

In the proposed real-time modeling method, the flow condition is updated using the estimation error (Fig.7):

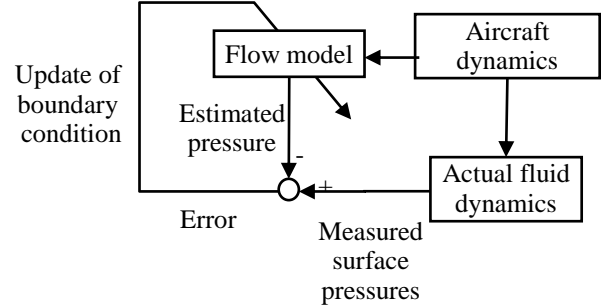


Fig.7 Proposed algorithm for real-time modeling

In this algorithm, the estimated flow condition is updated by changing the boundary conditions. As an example, the position where the Kutta condition is satisfied was varied, and the pressures of the flapping wing were calculated. Figure 8 shows the calculated pressure coefficient C_p for one stroke of the flapping motion below several positions corresponding to the Kutta condition. The assumed positions were the trailing edge and positions of 1% chord length from the trailing edge on the upper and lower surfaces. The pressure was estimated at the position of 30% chord length from the leading edge on the upper surface. Table 3 summarizes the calculation conditions.

Table3 Calculation conditions

Frequency [s ⁻¹]	1.00
Feathering motion [°]	10.0 sin(2πft)
Speed of free stream [m s ⁻¹]	5.00

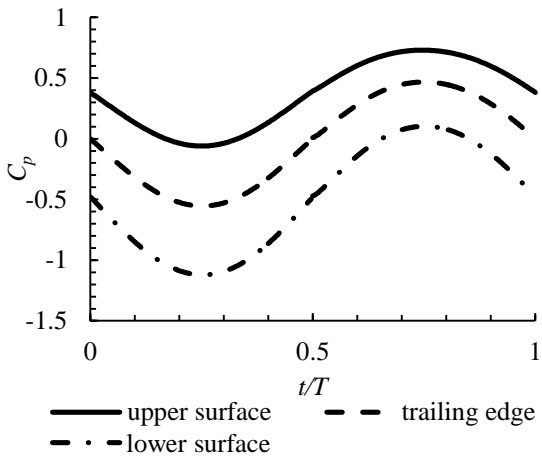


Fig.8 Time history of C_p under various boundary conditions

The flow condition can be adjusted significantly by changing the boundary conditions.

4. Experiments

The static pressures of the flat plate wing were measured and compared with the theoretical results. The wind velocity was 5 m/s. Figure 9 shows the used flat plate wing. The experimental parameters and used device are listed in Tables 4 and 5. The static pressure at the position of 20% chord length from the leading edge was measured.

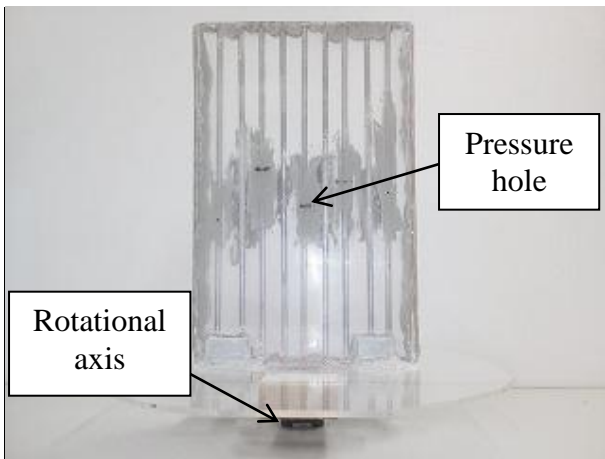


Fig.9 Experimental device

Table4 Wing parameters

Parameter	value
Chord [mm]	105
Span [mm]	160
Thickness [mm]	5.00

Table5 Specifications of pressure sensor

Maker	Sensirion
Model number	SDP-L025
Measurement range	± 62 [Pa]

The experimental results are shown in Fig. 9. The calculated values are also plotted in the figure.

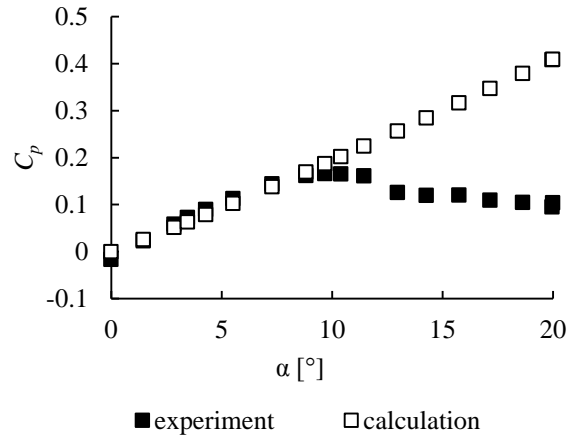


Fig.9 Results of experiment

The obtained results indicated that the theoretical value and measured value strongly agreed for a small angle of attack. However, when the angle of attack was large, the estimation errors became large. This error should be decreased by the proposed asymptotic method.

5. Conclusion

The flight dynamics of a flapping MAV affected by disturbances and wing deformation was modeled. The relations between the control performances and design parameters were investigated.

The basic concept for real-time modeling of the flow condition was proposed. In addition, the time history of the pressure on the flapping wing was calculated while varying the boundary conditions. The obtained results induced the use of the asymptotic algorithm in the proposed method.

In the future, a flight control system will be designed using the proposed real-time modeling method.

Reference

- [1] Taylor G K, and Thomas A L R. Dynamic flight stability in the desert locust *Schistocerca gregaria*, *The Journal of Experimental Biology*, 2003, 206, pp.2803-2829.
- [2] Sun M, and Xiong Y. Dynamic flight stability of a hovering bumblebee, *The Journal of Experimental Biology*, 2004, 208, pp.447-459.
- [3] Sunada S, Hatayama Y, and Tokutake H. Pitch, roll, and yaw damping of a flapping wing, *AIAA Journal*, 2010, 48, pp.1261-1265.
- [4] Tokutake H, Sunada S and Ohtsuka Y. Active control of flapping wings using wing deformation, *Transactions of the Japan Society for Aeronautical and Space Sciences*, 2009, 52, pp.98-103.
- [5] Sane S P and Dickinson M H. The control of flight force by a flapping wing: lift and drag production, *The Journal of Experimental Biology*, 2001, 204, pp.2607-2626.
- [6] Żbikowski R. On aerodynamic modelling of an insect-like flapping wing in hover for micro air vehicles, *Philosophical Transactions of the Royal Society of London Series A*, 2002, 360 (1791), pp.273-290.
- [7] Viieru D, Tang J, Lian Y, Liu H, and W Shyy. Flapping and Flexible Wing Aerodynamics of Low Reynolds Number Flight Vehicles, *AIAA*, 2006, 2006-503, pp.1-18.
- [8] Minotti FO. Unsteady two-dimensional theory of a flapping wing, *Physical Review E*, 2002, 66 (5), pp.1-10.
- [9] Ansari S A, Żbikowski R, and Knowles K. Non-linear unsteady aerodynamic model for insect-like flapping wings in the hover. Part 1: methodology and analysis, *Journal of Aerospace Engineering*, March 1, 2006, 220 (3), pp.169-186.
- [10] Ansari S A, Żbikowski R, and Knowles K. Non-linear unsteady aerodynamic model for insect-like flapping wings in the hover. Part 2: implementation and validation, *Journal of Aerospace Engineering*, March 1, 2006, 220 (3), pp.169-186.

Copyright Statement

The authors confirm that they, and/or their company or organization, hold copyright on all of the original material included in this paper. The authors also confirm that they have obtained permission, from the copyright holder of any third party material included in this paper, to publish it as part of their paper. The authors confirm that they give permission, or have obtained permission from the copyright holder of this paper, for the publication and distribution of this paper as part of the ICAS2012 proceedings or as individual off-prints from the proceedings.